

# Slow crack growth study of plaster using the double torsion method

M. Saadaoui<sup>a</sup>, P. Reynaud<sup>a,\*</sup>, G. Fantozzi<sup>a</sup>, F. Peronnet<sup>b</sup>, J.P. Caspar<sup>b</sup>

<sup>a</sup>INSA de Lyon — GEMPPM, UMR 5510, F 69621 Villeurbanne, France

<sup>b</sup>L.C.R. Lafarge, BP 15, F 38291 St Quentin Fallavier, France

Received 6 August 1999; received in revised form 25 August 1999; accepted 2 September 1999

## Abstract

Double torsion tests were performed to study slow crack growth (SCG) behavior of dry plaster. Preliminary, the fracture toughness  $K_{Ic}$  was measured, and higher value than that obtained with notched beams in bending test was found. This can be attributed to interactions between the surfaces of the initial crack in the DT samples. For SCG investigation, both load relaxation and constant loading tests were conducted. It is found that the relaxation method is not suitable for quantitative determination of the SCG law. Indeed, the load relaxation is very limited for dry samples and cannot be correlated to the crack propagation observed on the tensile surface. The constant loading results show that subcritical crack propagation occurs at  $K_I$  values lower than 30%  $K_{Ic}$ . This can be explained by the linkage of the main propagating crack with secondary cracks, the nucleation of which occurs at very low applied stresses. © 2000 Elsevier Science Ltd and Techna S.r.l. All rights reserved.

## 1. Introduction

Plaster is a porous brittle material characterized by a linear elastic macroscopic mechanical behavior when it is dry. It becomes non linear and its mechanical strength drops drastically in damp environment. Only few works have been published on the mechanical behavior of plaster, and in a large part they were focused on the variation of the mechanical properties with the porosity [1–4]. Takatsu et al. [5] have compared the fracture behavior of a set of plasters in different environments and recently, Coquard et al. [6] have proposed a thermodynamical approach of dry plaster fracture.

Very long service life is required for plaster in building applications, and the attempt of this study is to investigate its subcritical crack growth (SCG) behavior using the double torsion (DT) method [7–9]. Slow or subcritical crack growth of pre-existing cracks is one of the most important failure mechanism of brittle materials and it is generally attributed to stress induced corrosion in the crack tip. The crack growth rate  $V$  depends on the stress intensity factor,  $K_I$ , and the data are generally fitted to a power law:  $V = A(K_I)^n$ , where  $A$  and  $n$  are constant parameters, depending on the material and the environment, the knowledge of which allows life time prediction.

The DT method has received considerable attention as a direct method to determine the fracture toughness and SCG laws of materials, due to its simplicity and the possibility of conducting extensive crack propagation in a wide range of crack propagation rates under constant loading or in load relaxation test [7]. The sample geometry and the loading configuration are illustrated in Fig. 1. A compliance analysis [10] of the DT specimen indicates that the stress intensity factor  $K_I$  is independent of the crack length. The compliance  $C$  of a linear elastic solid, defined as the ratio of load point displacement to the load, varies linearly with crack length  $a$ :

$$C = Ba + D \quad (1)$$

where  $B$  and  $D$  are constants depending on the material. A theoretical value of  $B$  is given by:

$$B_{th} = \frac{3 \cdot W_m^2}{\mu \cdot W \cdot d^3 \cdot \Psi(d/W)} \quad (2)$$

with

$W_m$ : moment arm (Fig. 1),  
 $W$ : width of the specimen,  
 $d$ : thickness of the specimen,  
 $\mu$ : elastic shear modulus,  
 $\Psi$ : calibrating factor.

\* Corresponding author.

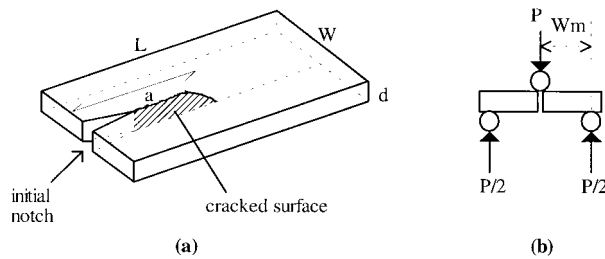


Fig. 1. Illustration of (a) the double torsion sample and (b) the loading configuration.

$K_I$  is given by:

$$K_I = P \cdot W_m \left( \frac{3}{W \cdot (1 - \nu) \cdot d^3 \cdot \Psi} \right)^{1/2} \quad (3)$$

where  $P$  is the applied load, and  $\nu$  is the Poisson's ratio.

The DT technique has been widely used for fracture mechanics studies of brittle materials. However, the authenticity of the test has been questioned [11] and the most important aspect was the effective constancy of the stress intensity factor  $K_I$  over the specimen length. Recently, a significant variation of  $K_I$  with crack length was observed in a 3Y-TZP ceramic [12], and a correction have been proposed to take it into account. Moreover, interactions between the propagating crack and the microstructure, and crack shielding mechanisms resulting in so called  $R$  curve behavior (crack growth resistance) lead to a shift of the  $V - K_I$  curve to higher values of  $K_I$  with increasing initial crack length [13–15].

Although it has been controversial, the double torsion method is very attractive. It allows rapid comparison of sub-critical crack growth behavior for different materials. Satisfactory results can be obtained for ceramic materials if care is taken to consider the materials specifications, especially  $R$  curve behavior [14,15]. The aim of this work is to check whether this method is suitable to investigate sub-critical crack growth in plaster, which is an important aspect of its fracture behavior.

## 2. Experimental procedure

### 2.1. Material and samples

Two grades of plaster denoted by PA and PB with respective densities of 1.6 and 1 g/cm<sup>3</sup> are used in this study. They were respectively obtained by hydration of  $\alpha$  and  $\beta$  hemihydrate powders Ca SO<sub>4</sub>0.5H<sub>2</sub>O with a ratio water to hemihydrate respectively of 0.4 and 0.8.

Rectangular plates with dimensions 300×180×10 mm<sup>3</sup> were performed and a notch of typically 100 mm in length was introduced in the center of each sample by saw cutting. Initial pre-crack, typically 10–20 mm in length, is obtained by loading the sample at a cross-head

speed of 0.1 mm/min. A good alignment of the specimen in the fixture constrains the propagating crack to the center of the sample.

### 2.2. Testing methods

The tests were performed at ambient temperature and 50% humidity, using a Schenck Trebel universal testing machine. The procedure was identical to that used by the authors for monolithic ceramics [12] and that gives a good agreement with results obtained using static and dynamic fatigue tests in bending [16]. Fracture toughness measurements were conducted by loading the pre-cracked samples at a cross-head speed of 1 mm/min. For subcritical crack growth investigations, both constant loading and relaxation tests were conducted. In the constant loading tests, the sample was subject to static loads and the crack growth rates were calculated as the ratio of the crack increment to the duration of loading. In the relaxation tests, the precracked specimens were subject to fast loading, followed by a subsequent stop of the cross-head at about 90% of the critical load. Assigning the load relaxation to the crack propagation, the load versus time curve allowed the determination of the  $V - K_I$  curve. The crack propagation rate,  $V$ , was calculated from the instantaneous load  $P$  and the corresponding load relaxation rate ( $dP/dt$ ):

$$V = -\frac{P_f}{P^2} \cdot \left[ a_f + \frac{D}{B} \right] \cdot \left( \frac{dP}{dt} \right) \quad (4)$$

where  $P_f$  is the final load and  $a_f$  the final crack length.  $B$  and  $D$  were obtained from a compliance calibration curve.

## 3. Results and discussion

### 3.1. Compliance analysis

A compliance versus crack length calibration  $C(a)$  was made using specimens with various crack lengths (Fig. 2). A linear behavior is observed within the range of the crack lengths investigated (80–200 mm), and the straight line fits to the experimental data resulted in values of  $B = 7.9 \times 10^{-5} \text{ N}^{-1}$  and  $D = 4.8 \times 10^{-6} \text{ N}^{-1}$ . Eq. (2) gives a theoretical value  $B_{th} = 1.7 \times 10^{-5} \text{ N}^{-1}$ . The difference between the theoretical and the experimental value is very important compared to the typical difference of 10% observed in ceramic materials and generally attributed to the deformation of the uncracked part of the sample.

### 3.2. Fracture toughness

The effect of the crack length,  $a$ , on the fracture toughness  $K_{Ic}$  was investigated. Typical results for the

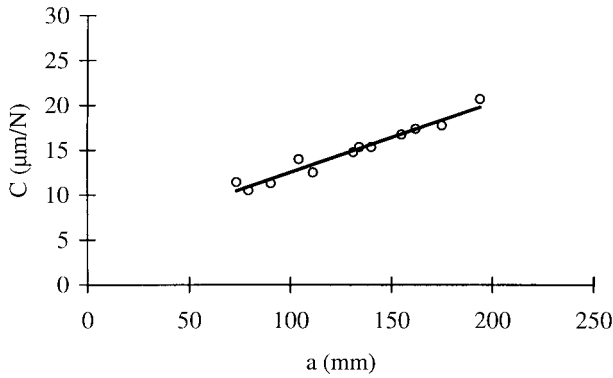


Fig. 2. Compliance versus crack length for the PB plaster.

DT test are obtained, as shown in Fig. 3. The toughness is constant over the range of crack lengths 95–150 mm, and decreases when the crack front approaches the sample edges.

Typical values of the maximum load and the measured fracture toughness are listed in Table 1. For comparison, the maximum load of a damp sample of the PB plaster, denoted by PBH, is also reported. The toughness is higher by a factor 4 for the dense plaster PA. For comparison, the fracture toughness was also measured in three-points bending test using straight-notched specimens with dimension  $20 \times 40 \times 180 \text{ mm}^3$  and a 135 mm span between supports. Values of 0.12 and  $0.35 \text{ MPa m}^{1/2}$  were obtained, respectively, for PB and PA dry plasters. The difference between the results can be attributed to interactions between the surfaces of initial pre-crack in the DT sample. Indeed, both the materials show rising  $R$  curve behavior (Fig. 4) and the DT results correspond to the plateau value of the  $R$  curve since the initial pre-crack length exceeds the crack propagation (about 2 mm) over which the  $R$  curve is rising.

The influence of the cross-head speed on  $K_{IC}$  was also investigated and no significant change in  $K_{IC}$  was observed when the cross-head speed was increased from 0.01 to  $10 \text{ mm mn}^{-1}$ .

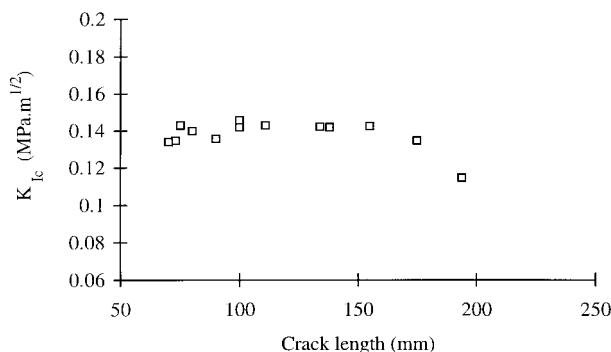


Fig. 3. Fracture toughness versus crack length for the PB plaster.

Table 1

Maximum load and fracture toughness in DT testing

Material	PA	PB	PBH
$P_c$ (N)	125	40	30
$K_{IC}$ ( $\text{MPa m}^{1/2}$ )	0.5	0.14	–

### 3.3. Slow crack growth behavior

#### 3.3.1. Load relaxation tests

In addition to dry samples, a damp sample of the PB plaster was tested. Linear behavior was observed during loading of dry samples whereas substantial deviation from linearity occurred for the damp sample. Fig. 5 shows typical load relaxation curves. It can be seen that the relaxation is very limited for dry sample of PB. At 95% of the critical load,  $P_c$  (at which critical crack propagation occurs) the total load drop is only of 3 to 4 N although substantial crack growth up to 10 mm occurred. It is to note that multiple crack propagation and branching was observed on the tension surface. For the dense material, PA, the relaxation is more important, typically 12 to 15 N at initial load of 110 N. The load drop and the crack extension increase significantly during relaxation of a damp sample.

Fig. 6 shows the  $V-K_I$  curves resulting from the load relaxation. For PB dry samples, the total range of  $K_I$  measured is very small and an apparent threshold value very close to the fracture toughness  $K_{IC}$  is observed. Although the method is not applicable to the damp sample due to its non linear behavior, an apparent  $V-K_I$  curve was determined for qualitative comparison with the dry sample. It can be seen (Fig. 6) that the curve is shifted to lower stress intensity factor values and the total range of the measured  $K_I$  is larger. Similar results have been reported by Takatsu et al. [5]. However, quantitative SCG law cannot be deduced from the relaxation curves as it will be shown below.

As the relaxation was very small for the dry PB sample, the effect of extraneous relaxations from the loading

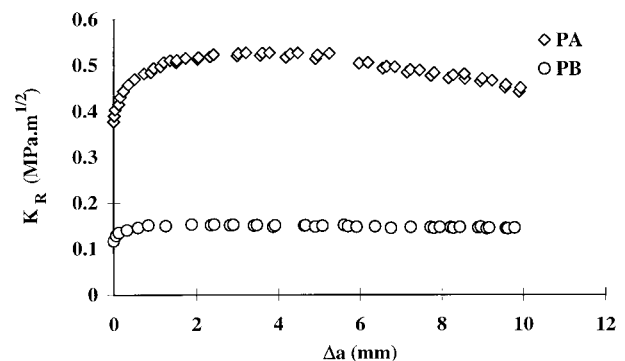


Fig. 4.  $R$  curves obtained in three-points bending at a cross-head speed of  $0.005 \text{ mm/min}$  (relative initial notch depth 0.5).

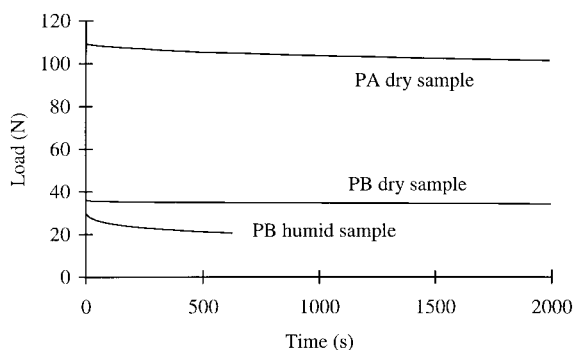


Fig. 5. Load relaxation curves for dry PA, PB, and for a damp PB sample.

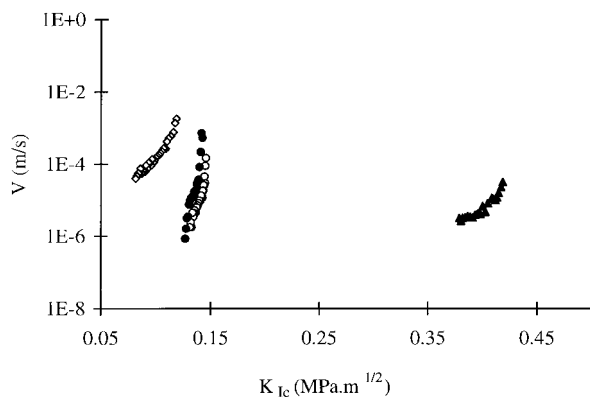


Fig. 6.  $V$ – $K_I$  curves resulting from load relaxation for dry PA (▲), PB (○, ●), and for a damp PB sample (◇).

fixture and the testing machine cannot be neglected. To take them into account, a set of uncracked plates were loaded in the same condition as the precracked plates and their relaxation was recorded. Surprisingly, the relaxation curve was identical to that recorded for a precracked sample (Fig. 7). This implies that the subcritical crack propagation of the main crack observed in the precracked specimen cannot be correlated to the load relaxation. Thus, relaxation tests are not suitable to determine slow crack growth behavior of plaster.

### 3.3.2. Constant loading test

Constant loading tests were performed on a unique dry PB sample within the range of crack lengths where  $K_{Ic}$  is constant. The extension of the main crack,  $da$ , was optically measured allowing precise determination of the crack propagation rate,  $V = da/dt$ . The results plotted as  $V$  versus the relative stress intensity factor  $K_I/K_{Ic}$  are shown in Fig. 8. It can be seen that the crack propagation rate decreases rapidly with the stress intensity factor in the vicinity of the fracture toughness, then remains nearly constant. In contrast with the relaxation test, no threshold was observed. Subcritical crack propagation occurred at  $K_I$  values lower than 30%  $K_{Ic}$  and the crack growth rates are several orders of magnitude higher than those deduced from load relaxation.

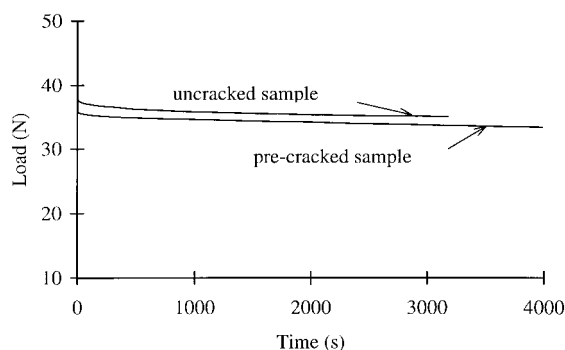


Fig. 7. Load relaxation curves for precracked and unnotched dry samples of PB plaster.

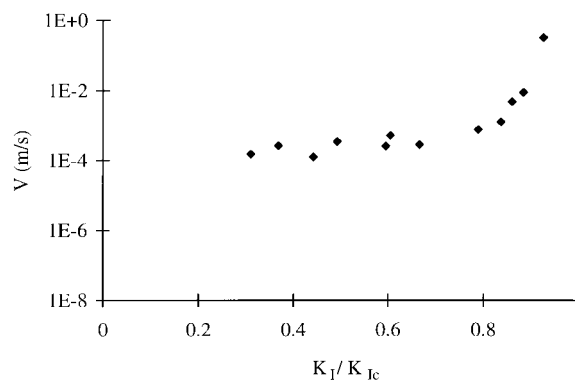


Fig. 8.  $V$ – $K_I$  curves resulting from constant loading tests of PB plaster.

Observation of the tensile surface of the sample at the end of each static test showed that substantial secondary cracking occurs around the main crack, and the crack propagation seems to occur by the interlink of the main propagating crack with secondary cracks. Crack nucleation from pores can occur at low applied stresses assisted by the stress concentration due either to the main crack and to the important inherent porosity. It may also be attributed to low surface energy due to local heterogeneity. Indeed, the observation of fracture surface of plaster shows that crack propagation occurs essentially by decohesion of gypsum microcrystals. A certain fraction of them may have low bond energy and constitute sites for microcrack nucleation and growth at low applied stresses.

One must be careful in the interpretation of the results, according to the particularities of the plaster (microstructure, high porosity, crystal orientation at the surface) and to the nature of the DT method. It should be noted that the substantial secondary cracking and branching observed have not been taken into account, and the crack front has been assumed constant. The main crack propagation is not continuous and the crack propagation rate is not uniform. So, calculation of  $V$  as the ratio of the crack extension to the loading duration may lead to erroneous value. Moreover, in the DT

samples, the crack front is not straight and the crack propagation occurs essentially in the vicinity of the tensile surface. In the case of plasters, the observed crack propagation may not be representative of the bulk of the material due to crystal orientation effects at the surface of the sample. Further work will be done using straight crack front samples with in situ crack propagation measurements to confirm the previous results and to investigate the SCG mechanisms which are probably identical to those controlling the fracture of damp plasters.

#### 4. Conclusion

Slow crack growth behavior of plaster was investigated by the double torsion technique (DT). Preliminary fracture toughness measurements give reproducible  $K_{Ic}$  values slightly higher than those obtained from notched beams in bending tests.

One must be careful in the interpretation of the SCG results. The load relaxation method is not suitable for quantitative study of SCG behavior of both dry and damp plaster. Indeed, the load relaxation is very limited in dry samples especially for the high-porosity material and cannot be correlated to the subcritical crack propagation observed on the tensile face at the end of the test. For damp plaster, the behavior deviates strongly from the linear elasticity required to apply this method.

The constant loading results show that subcritical crack propagation occurs at  $K_I$  values lower than 30%  $K_{Ic}$ . This can be explained by the interlink of the main

propagating crack with secondary cracks, the nucleation of which occurring at very low applied stresses. These results have to be further confirmed using other sample geometry with in situ crack propagation measurements.

#### References

- [1] I. Soroka, P.J. Sereda, *J. Am. Ceram. Soc.* 51 (1968) 337–340.
- [2] G. Vekinis, M.F. Ashby, P.W.R. Beaumont, *J. Mater. Sci.* 28 (1993) 3221–3227.
- [3] K.K. Phani, *Am. Ceram. Soc. Bull.* 65 (1986) 1584–1586.
- [4] P. Coquard, R. Boistelle, L. Amathieu, P. Barriac, *J. Mater. Sci.* 29 (1994) 4611–4617.
- [5] M. Takatsu, K. Shimomura, I. Takahashi, T. Ono, *Gypsum Lime* 173 (1981) 149–155.
- [6] P. Coquard, J. Boistelle, *J. Mater. Sci.* 31 (1996) 4573–4580.
- [7] J.O. Outwater, M.C. Murphy, R.G. Kumble, J.T. Berry, in: *Fracture toughness and slow-stable cracking*, ASTM STP 559, 1974, pp. 127–138.
- [8] E.R. Fuller, in: *Fracture mechanics applied to brittle materials*, ASTM, STP 678, 1979, pp. 3–18.
- [9] B.J. Pletka, E.R. Fuller, B.G. Koepke, in: *Fracture mechanics applied to brittle materials*, ASTM, STP 678, 1979, pp. 19–37.
- [10] D.P. Williams, A.G. Evans, *Journal of Testing and Evaluation* 1 (1973) 264–270.
- [11] D.K. Shetty, A.V. Virkar, M.B. Harward, *J. Am. Ceram. Soc.* 62 (1979) 307–309.
- [12] J. Chevalier, M. Saadaoui, C. Olagnon, G. Fantozzi, *Ceram. Int.* 22 (1996) 171–177.
- [13] A. Okada, N. Hirotsaki, *J. Am. Ceram. Soc.* 73 (1990) 2095–2096.
- [14] F. Mignard, Ph.D. thesis, INSA de Lyon, 1995.
- [15] M. Ebrahimi, J. Chevalier, M. Saadaoui, G. Fantozzi, *Frac. Mech. Ceram.* 13, in press.
- [16] J. Chevalier, C. Olagnon, G. Fantozzi, B. Cales, *J. Am. Ceram. Soc.* 78 (1995) 1889–1894.